DETERMINATION OF SENSORY MOTOR COORDINATION PARAMETERS FOR A ROBOT VIA TELEOPERATION

MARK EDWARD CAMBRON
Department of Engineering
Western Kentucky University
Bowling Green, KY 42101

RICHARD ALAN PETERS II
Center for Intelligent Systems
Vanderbilt University
Nashville,TN 37235

Abstract

This paper proposes a method for the determination of Sensory-Motor Coordination (SMC) parameters through the teleoperation of a humanoid robot designed for human-robot interaction. It is argued that SMC in a complex environment must be acquired rather than programmed. It is demonstrated that the acquisition of SMC parameters through teleoperation during a task can enable a robot to determine the category of the outcome of the task during autonomous operation. The outcome can be determined without the a priori programming by a person of sensory cues. That is, the robot learns its own sensory cues.

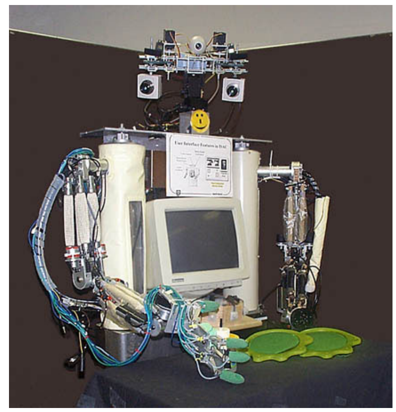

Figure 1: Vanderbilt's humanoid robot: ISAC.

1 Introduction

Researchers at the Intelligent Robotics Laboratory at Vanderbilt University have been developing a humanoid robot, ISAC, over the past several years (Figure 1). The robot was designed expressly for research in human-robot interaction [1]. ISAC's control architecture is an agent-based, hybrid deliberative-reactive system. Like many behavior-based robots, ISAC's complex behaviors result from the interaction of independent computational modules that operate asynchronously in parallel [2].

To interact with people in a human-centered environment a robot must exhibit intelligent behavior. This requires the ability to adapt its actions to changing environmental conditions. A robot estimates these conditions through sensing; therefore, intelligent behavior requires the ability to coordinate actions with the responses of sensors. That is, intelligent behavior requires *sensory motor coordination* (SMC).

At its lowest level SMC is a reflex, a direct motor response to sensory stimulation. If reflexes are determined *a priori* by the robot designer the result is typically inefficient at best, or completely wrong at worst. It it is difficult if not impossible, for the designer to anticipate the sensory information available to the robot which, in an unforeseen situation, will be salient for action selection. To be robust, the robot should acquire its own reflexes.

This paper reports a test of the hypothesis that SMC can be acquired through teleoperation then used for autonomous operation of the robot. The goal is that, during repeated teleoperation trials of a task, if the robot records all of its sensory signals, then through statistical analysis, those sensory-motor couplings which accompany purposeful motion can be identified. The SMC acquisition algorithm determines which parts of that information are significant and should be used, and which are insignificant and can be ignored. The significant information can be used to find exemplars of the SMC for the behaviors that comprise the task. Different exemplars then characterize different categories of tasks. During a subsequent autonomous execution of the task, the SMC information can be compared to the exemplars to determine the category of the robot-environment interaction.

2 Sensory Motor Coordination

Sensory-Motor Coordination (SMC) underlies the physical behavior of an animal in response to its environment. More than a response, SMC is a feedback loop that changes both the animal and the environment. An animal's motions are caused by muscle contractions. These contractions are elicited by electro-chemical signals that are generated by circuits of motor neurons. When the animal moves, it causes a relative shift in the environment. As the environment shifts, energy patterns sweep across the animal's sensory organs. Sensory organs are transducers that, in effect, transform external, spatio-temporally dynamic energy fields into electro-chemical signals carried by circuits of

0-7803-7087-2/01/ $10.00 © 2001 IEEE

sensory neurons internal to the animal. These sensory signals (more or less directly) modulate the signals in the original motor circuits. Thus, an animal senses the environment and acts. The action changes the environment relative to the animal; the animal senses those changes and acts accordingly.

SMC is fundamental to behavior based robotics; it underlies the concept of basic behavior. Moreover, it forms a foundation for higher level learning and perception. In particular, the categorization of sensory stimuli can be accomplished through SMC [3]. A mobile agent can learn the sensory patterns that correspond to an obstacle by associating stimuli with its motor responses, as when a characteristic stimulus pattern routinely accompanies the sudden inability to move. Similarly, as Pfeifer has demonstrated, an agent can learn to distinguish between objects that it can manipulate and those which it cannot [4]. If an internal indicator of a need (a drive or a goal) having been met accompanies a set of actions performed in the presence of specific stimuli, those stimuli can be recognized subsequently as beneficial to the agent (*e.g.* an energy source – food). Recent experiments by Pfeifer and others have demonstrated that such SMC events (temporal coincidences of sensory signals and motor actions) can be used to learn classifications of objects and events in the environment more easily and more accurately than can traditional machine sensing strategies such as model-based vision [5, 6].

There are at least two approaches that might enable a robot to acquire Sensory-Motor Coordination. One is to set up a reinforcement learning scheme which allows the robot to move randomly. As the robot wanders, the sensory-motor events that lead to purposeful motion are reinforced. Those couplings that do not are suppressed. Eventually, the robot would learn useful SMC. A second approach takes advantage of the fact that a robot can be teleoperated. When a person teleoperates a robot, the person's SMC (in effect) causes the robot to act purposefully. That is, the teleoperator watches the robot and based on his or her own observations, controls the motion of the robot. If during such teleoperation the robot records its own sensory information, it could, perhaps, associate its own sensory signals with particular actions. This approach would bootstrap the process of acquiring SMC and is analogous to a parent helping a child to walk by holding her or his hand while giving encouragement. The child still must learn how to control her actions, but the parent's assistance and encouragement abets the process.

3 Methods and Procedures

In previous work the researchers found that during autonomous operation ISAC would often fail in an attempt to grasp an object. It was found that many failures occurred because the grasp axis of the hand[1] was not aligned with the principal axis of the object. The failure rate could be reduced if after reaching for an object, but prior to grasping, ISAC could determine that its hand were incorrectly aligned. Through SMC the robot could detect situation and adjust its wrist position accordingly.

The idea that SMC might be acquired by a robot through teleoperation, led the researchers to an experiment which enabled ISAC to detect pregrasp misalignment. ISAC was controlled by the experimenter (Cambron) to reach for and attempt to grasp a fixed vertical pole. Repeated trials were run using three categories of reach outcome prior to grasping: (1) The hand was correctly aligned -- the grasp axis was parallel to the principal axis of the pole. (2) The hand was tilted $+10°$ with respect to the pole. (3) The hand was tilted by $-10°$. Trials of category 1 nearly always resulted in a successful grasp. Trials of category 2 and three nearly always led to a failure to grasp the pole. Values $\pm 10°$ were chosen by the experimenter empirically to make grasp failure likely. The experiment enabled ISAC during autonomous operation to recognize each of the reach outcomes prior to grasping. If the outcome were incorrect the robot would adjust its position.

SMC Parameter Acquisition. SMC parameters were acquired as follows:

1. Teleoperated trials of the same task were run repeatedly with each of the possible outcomes represented equally. All sensory signals were recorded.

2. The signal set for each trial was partitioned (in time) into episodes by motor state changes, which served as temporal markers.[2] For any given trial of the task the sensory signal is a multimodal vector denoted:

$$\vec{S}(t;r,p) = \left[\ \vec{S}_1(t;r,p)\ \middle|\ \cdots\ \middle|\ \vec{S}_M(t;r,p)\ \right] \quad (1)$$

   where subvector $\vec{S}_n(t;r,p)$ $(n = 1, \ldots, M)$ is the signal from sensor n, t is time, r is the trial number, and p is the episode number.[3]

3. For each episode, p, the signals from each trial, r, were resampled to normalize them in

[1]The grasp axis lies in the palm perpendicular to the fingers.

[2]An episode is the set of sensory signals recorded during the time between successive motor state changes.

[3]Some of the signals (*e.g.*, force) are vector-valued with multiple scalar components, while others (*e.g.*, proximity) have only one component. Nevertheless, the signal from sensor n is denoted by the vector $\vec{S}_n(t)$. Vector-valued signals have scalar signal components which are denoted S_j (without the arrow). There are M vector signals $\vec{S}_n(t)$ – one per sensor – and a total of N scalar signals S_j where $N > M$.

duration and sampling rate. Then for a specific p scalar signal $S_j(t;r,p)$ contained K_p samples in each trial, r. We assume that the number of samples exceeds the number of signals, that $K > N$.

4. Within episode p scalar signal $S_n((t;r,p))$ from a single sensor was compared across all trials. That is, the set

$$\{S_n((t;r,p))\}_{r=1}^{N} \qquad (2)$$

was analyzed for fixed p and fixed n across all trials, r. The analysis identified those sensors whose signals were similar in each trial. Those modalities were considered to be salient to the episode. Their signals were retained. Those sensors whose signals varied randomly across the trials were considered to be uninformative to the task during that episode; their signals were not considered further.

5. The retained signals were averaged across all trials. That is, within episode p, the scalar signals, $S_n((t;r,p))$ from sensor n (one for each trial, r) were averaged time-wise over r. The result was a set of characteristic signals $\chi_n(t;p)$, one for each relevant sensor and for each episode.

The signals recorded during the experiment are listed in Table 1.

Table 1: Signals measured during teleoperation.

$\vec{S}_1$:	Arm positions (X,Y,Z,roll,pitch,yaw)
$\vec{S}_2$:	Finger Positions
$\vec{S}_3$:	6-axis Force-Torque sensor output
$\vec{S}_4$:	Proximity sensor 1 output
$\vec{S}_5$:	Proximity sensor 1 output
$\vec{S}_6$:	Finger touch sensor 1
$\vec{S}_7$:	Finger touch sensor 2

The grasping experiment used several behaviors: object fixation, visual servoing, and grasp object (Figure 2).

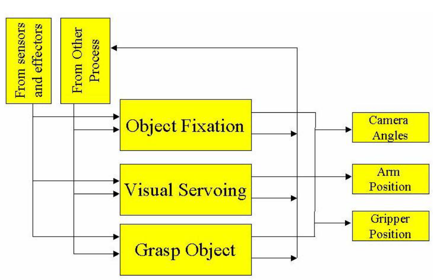

Figure 2: Behaviors in grasping experiment.

Learning SMC. The motor control sequence in a teleoperated trial determined the motor events (times of transition between continuous motor operation states) that partitioned the sensory signals into episodes [7]. During teleoperation these transitions were initiated by the operator. Episode boundaries are discernible not only by motor events but also from sensor data. A sensory event that precedes a motor state change can be used by the robot to trigger the state change during autonomous operation. For example, when the hand hits an object there is a significant change in the total force, F_{total}, or total torque, F_{total}. In response to this event the robot should stop moving.

To find the significant sensory-motor data all the signals were processed. Once the SMC motor events were determined, the signals were resampled, filtered, and normalized.

Signal Warping. The signal set from each teleoperated trial is partitioned into the same number of episodes, but the durations of these vary. The determination of the characteristic signal that reliably precedes or follows a particular motor state change requires a comparative analysis of the signals from a given sensor over several trials. This, in turn, requires that the signals have the same duration (and the same number of samples) within a specific episode over all the trials. Since the duration of episode p varies from trial to trial, the entire vector signal $\vec{S}(t;r,p)$ must be resampled so that the episode durations match and are thus independent of the trial number r.

The episode durations were normalized by interpolating the signal by a factor of U followed by decimating the output of the interpolator by a factor of D. The result was smoothed by a 3^{rd} order difference filter.

Characteristic Signals. After R trials for each of the three hand angle outcomes $\theta \in \{0°, 10°, -10°\}$ were completed three characteristic signals $\vec{\chi}^{\,0}$, $\vec{\chi}^{\,10}$, and $\vec{\chi}^{\,-10}$ were computed. Each scalar component of these vector signals is the amplitude-normalized time-wise average over all trials with outcome θ of the jth episode-duration-normalized scalar signal $S_j^{\theta}(t)$.(Say that quickly.) For each outcome, θ, and each episode, p, let

$$\chi_j'^{\theta}(t;p) = \frac{1}{R}\sum_{r=1}^{R} S_j^{\theta}(t;r,p), \qquad (3)$$

where each S_j^{θ} was previously duration normalized. Each of these scalar characteristic signals is amplitude normalized with respect to its energy norm to get

$$\chi_j^{\theta}(t;p) = \frac{\chi_j'^{\theta}(t;p)}{\|\chi_j'^{\theta}(t;p)\|} \qquad (4)$$

The characteristic vector signal for outcome θ and episode p is then[4]

$$\vec{\chi}^{\theta}(t;p) = \left[\ \chi_1^{\theta}(t;p) \ \middle| \cdots \middle| \ \chi_N^{\theta}(t;p) \ \right] \quad (5)$$

4 Category Estimation

A signal, $\vec{S}(t;p)$, collected during autonomous operation is referred to as an observed signal. $\vec{S}(t;p)$ is the vector of N scalar sensor signals from episode p (resampled and amplitude normalized). To facilitate analysis the signal vector notation has been changed to a signal matrix notation. For a given episode, p, signal $S_j(t;p)$ contains K_p samples. Write the samples in each $S_j(t;p)$ as a column vector $\mathbf{S}_j(p)$. Let

$$S(p) = [\ \mathbf{S}_1(p) \quad \mathbf{S}_2(p) \quad \cdots \quad \mathbf{S}_N(p)\ ]. \quad (6)$$

Then $S(p)$ is a $K_p \times N$ matrix where the row index corresponds to time and the column index to sensor modality.

Each characteristic signal for episode p from outcome θ has a matrix of the same dimensions:

$$\chi^{\theta}(p) = [\ \chi_1^{\theta}(p) \quad \chi_2^{\theta}(p) \quad \cdots \quad \chi_N^{\theta}(p)\ ]. \quad (7)$$

Several methods for comparing the observed signal to the three characteristic signal were tested. Each of the N sensor scalar signals $\mathbf{S}_j(p)$ for episode p are vectors in the K_p-dimensional space,

$$\mathbf{S}_j(p) \in \Re^{K_p}, \quad (8)$$

as are the $3N$ characteristic signals $\chi_j^{theta}(p)$. For each θ the set of N characteristic signals span an N-dimensional (or less) subspace of the K_p-dimensional signal space. Thus there is one subspace per category. Within this vector space / subspace context the category of the observed signal is estimated.

Cross-Correlation at Time Lag 0. The cross-correlation at time lag 0 of observed signal $S(p)$ with characteristic signal $\chi^{\theta}(p)$ is given by the $N \times N$ matrix

$$C(p,\theta) = \chi^{\theta}(p) S(p)^T \quad (9)$$

Element (i,j) of $C(p,\theta)$ (denoted $C_{ij}(p,\theta)$) is the temporal cross-correlation of $S_i(t;p)$ with $\chi_j^{\theta}(t;p)$. In terms of vector spaces, it is the projection of $\mathbf{S}_i(p)$ onto $\chi_j(p)$ (Figure 3). For a given θ, $|C_{ij}(p,\theta)|$ is a metric that indicates the similarity between observed sensor signal i and characteristic signal j.

The trace of the cross-correlation matrix is a measure of how well each sensor sub-signal in the observed signal matches the corresponding subsignal in the characteristic signal. The average correlation, $E^{\theta}(p)$, between them is the trace of the cross correlation matrix divided by the number of signals.

$$E^{\theta} = \frac{1}{N} \ \mathrm{trace}\, \{Cp, \theta\} \quad (10)$$

Table 2 shows the results of Equation 9 in predicting the correct category. When using only the force and the torque data the correct category was selected 80% of the time. When the Z-position signal was included the results did not change. However, when both the Y- and Z-positions were included, the results improved to 86.667%.

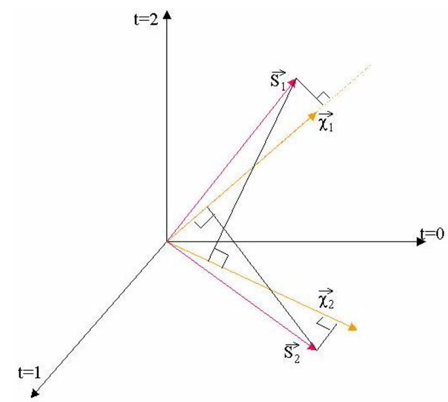

Figure 3: Signal space for cross-correlation.

Table 2: Results of Correlation Method at lag 0.

	Correct	Incorrect
6 Dimension	80.00%	20.00%
7 Dimension	80.00%	20.00%
9 Dimension	86.67%	13.33%

Cross-Correlation with Non-Zero Time Lags. To correct for possible time shifts between the observed and characteristic signals nonzero lag cross-correlations were computed. Table 3 shows the results of the cross-correlation analysis where each $C_{ij}(p,\theta)$ was the maximum over over the lag values. There was no difference in the percent of correct outcomes between the zero-lag case and the non-zero lag case.

Correlation less Auto Correlation. The cross correlation approach described above used only the correlations between similar sensor signals. That is, the only values used were $C_{ii}(p,\theta)$. To include the $C_{ij}(p,\theta)$, $j \neq i$ coefficients in the test, the cross-correlation matrix, $C(p,\theta)$ was

[4]To distinguish between categories the superscript θ is used. When the statement is true for all categories no superscript is used.

Table 3: Results of correlation method.

	Correct	Incorrect
6 Dimension	80.00%	20.00%
7 Dimension	80.00%	20.00%
9 Dimension	86.67%	13.33%

compared to the autocorrelation matrix, $R(p, \theta)$ of the characteristic signals.

$$R(p, \theta) = \chi^{\theta}(p) \chi^{\theta}(p)^T \tag{11}$$

the mean-square difference between $\chi^{\theta}(p)$ $C(p, \theta)$ will be minimum for the characteristic signal that correlates with the observed signal most like it correlates with itself.

$$Q^{\theta} = \sum_{j=1}^{K} \sum_{i=1}^{K} |R_{ij}(p, \theta) - C_{ij}(p, \theta)|^2 \tag{12}$$

The results of this approach were identical to those of the previous two. (Table 4.)

Table 4: Results of correlation less auto-correlation at lag 0.

	Correct	Incorrect
6 Dimension	80.00%	20.00%
7 Dimension	80.00%	20.00%
9 Dimension	86.67%	13.33%

Singular Value Decomposition. For each outcome θ the set of N characteristic signals $\{\chi_j^{theta}(p)\}_{j=1}^{N}$ span an N-dimensional (or less) subspace of the K_p-dimensional signal space. If these subspaces are distinct then the projection of the observed signal set $\{\mathbf{S}_j(p)\}_{j=1}^{N}$ onto each of them can perhaps be used to distinguish between the outcomes. The singular value decomposition (SVD) of the characteristic spaces facilitates this type of subspace analysis. The SVD for outcome θ describes that characteristic signal subspace in terms of an orthonormal basis set. The observed signal vectors, $\mathbf{S}_j(p)$ are projected onto this basis set to measure the degree to which the observed signal lies in the characteristic signal subspace for outcome θ (Figure 4).

$$\Psi_{\theta} = \sum_i \sum_j W_{\theta}^2(i, j) \tag{13}$$

The results listed in Table 5 reflect a poor performance compared to the correlation methods.

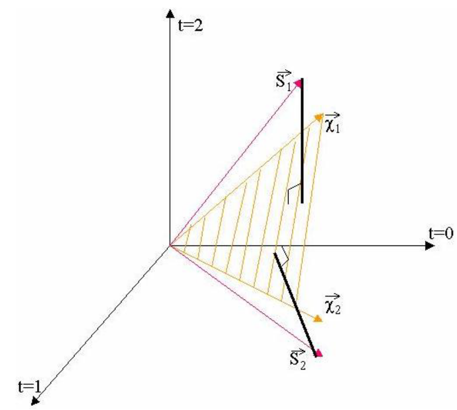

Figure 4: Signal space for SVD.

Table 5: SVD method.

	Correct	Incorrect
6 Dimension	73.33%	26.67%
7 Dimension	73.33%	26.67%
9 Dimension	73.33%	26.67%

Neural Network. Another method for used for category determination was a neural network trained to map the characteristic signals to the correct categories. A multi-layer perceptron network was implemented. The network is trained using using the backward error propagation (backprop) algorithm. The network works by partitioning the K dimensional space into 3 subspaces each of which contains the N-vector characteristic signal set for one outcome (Figure 5).

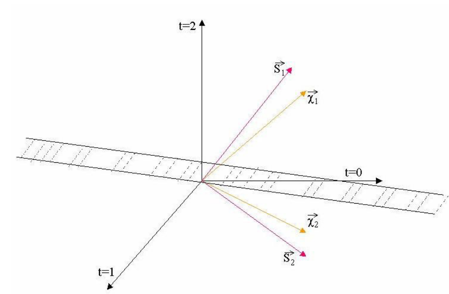

Figure 5: Signal space for neural network.

Table 6 shows that the network using the 7-signal characteristic set gave the correct result 93.75% while giving the wrong result 6.25%. Thus, the neural net provides the best classification.

Effect of Noise An experiment was conducted on the effect of noise on the quality of the characteristic signals $\vec{\chi}^{\theta}(t;p)$. White gaussian noise was added to each characteristic signal. The noise was constructed to be of the same dimensionality and

Table 6: Neural network results.

	Correct	Incorrect
6 Dimension	87.50%	12.50%
7 Dimension	93.75%	6.25%
9 Dimension	87.50%	12.50%

energy as the signals used to construct the characteristic signals. Figure 6 shows the results percentage noise versus the percentage correct using the Cross-Correlation at Time Lag 0 method. The figures shows the the results drop off dramatically once the noise gets larger than 30%.

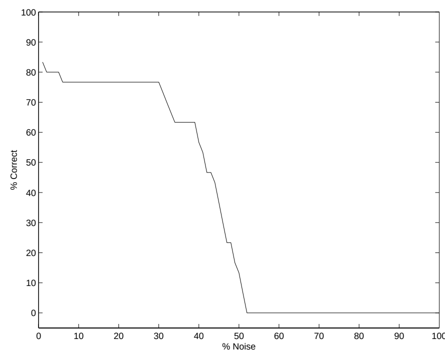

Figure 6: Noise curve.

Exemplars Figure 7 shows the results of comparing the number of exemplars used to calculate the characteristic signal versus the percentage correct using the Cross-Correlation at Time Lag 0 method described previously in this chapter. Three curves are presented.

The "best" curve shows using the signals which have the highest correlation with the 3 characteristic signals. As expected this curve gave results that ranged from 73% to 86.67%. The "random" curve shows the results of taking all combinations for the 3 characteristic signals. The "worst" curve used the lowest correlation with the 3 characteristic signals. The results for the "worst" produced results that started much lower (13.33%).

5 Conclusions

In this paper a method for acquisition of SMC parameters via teleoperation was presented. The robot was able to use these parameters to correctly estimate the correct category during autonomous operation of the task by the humanoid robot. It was shown that the robot could determine its own sensory cues.

This work has been partially funded by a grant from NASA through the Research Institute for Computing and Information Systems. For more information, please visit our web page at http://shogun.vuse.vanderbilt.edu.

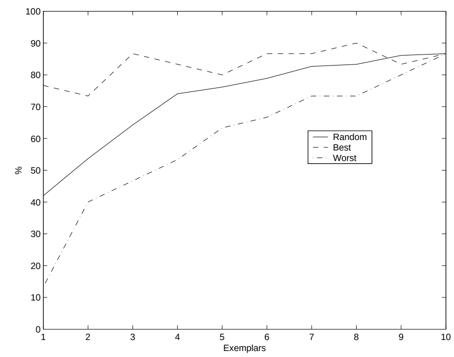

Figure 7: Exemplars curve

References

[1] K. Kawamura, R. Peters II, D. Wilkes, W. Alford, and T. Rogers, "Isac: Foundations in human-humanoid interaction," *IEEE Intelligent Systems*, vol. 15, pp. 38–45, July/August 2000.

[2] R. Peters II, D. Wilkes, D. Gaines, and K. Kawamura, "A software agent based control system for human-robot interaction," in *Proceedings of 2^{nd} International Symposium on Humanoid Robotics (HURO '99)*, (Tokyo, Japan), Oct. 1999.

[3] C. Scheier and R. Pfeifer, "Classification as sensory-motor coordination," in *Proceedings 3rd European Conference on Artificial Life*, pp. 656–667, 1995.

[4] R. Pfeifer, "Embodied system life," in *Proceedings of the International Symposium on System Life*, Sept. 1997.

[5] D. Lambrinos and C. Scheier, "Building complete autonomous agents: a case study on categorization," in *Proceedings of the IEEE/RSJ International Conference on Intelligent Robots and Systems*, (Osaka, Japan), Nov. 1996.

[6] R. Pfeifer and C. Scheier, "Representation in natural and artificial agents: an embodied cognitive science perspective," *Zeitschrift fr Naturforschung*, vol. 53, no. 7-8, pp. 480–503, 1998.

[7] P. Cohen, "Learning concepts by interaction," Tech. Rep. 00-52, University of Massachusetts, Computer Science Department, Amherst, MA, 2000.